

# INTERNATIONAL SOCIETY FOR SOIL MECHANICS AND GEOTECHNICAL ENGINEERING



*This paper was downloaded from the Online Library of the International Society for Soil Mechanics and Geotechnical Engineering (ISSMGE). The library is available here:*

<https://www.issmge.org/publications/online-library>

*This is an open-access database that archives thousands of papers published under the Auspices of the ISSMGE and maintained by the Innovation and Development Committee of ISSMGE.*

# Undrained monotonic and cyclic shear behaviour of saturated sand under wide range of confining stresses

Le comportement non-drainée cyclique et monotonique du sable saturé sous une gamme grande de pression effective

M.Hyodo – Professor, Department of Civil Engineering, Yamaguchi University, Ube, Japan  
N.Aramaki – Assistant Professor, Department of Civil Engineering, Sojo University, Kumamoto, Japan

**ABSTRACT:** Since for weak grained soils particle crushing occurs even at low stresses, the authors carried out tests on a hard grained sand over a wide range of stresses to distinguish non-crushing and crushing behaviours. Samples were therefore sieved not only before and after but also at intermediate stages of undrained monotonic and cyclic shear tests at low and high confining stresses to establish the degree of crushing that had occurred. In addition this series of tests can draw on the previous large volume of low stress liquefaction data on the same hard grained sands, and thus allow contrasts to be made between the cyclic strength characteristics in the crushing and non-crushing regions.

**RÉSUMÉ:** Cette recherche traite de l'effet de la compressibilité et le concassage du sol sur la résistance non drainée cyclique et monotonique. D'après les recherches précédentes il est évident que la densité initiale et la pression effective étaient importantes pour le comportement cyclique. Il y avait du concassage des particules pendant ces essais non drainés. Vu que le concassage des particules des sables avec les grains faibles se passe même à effort bas, on a décidé d'essayer du sable avec des grains durs utilisant des efforts très divers pour distinguer entre le comportement avec concassage et sans concassage. Les échantillons ont été tamisés avant, après et à des phases intermédiaires des essais pour établir le degré de concassage.

## 1 INTRODUCTION

In 1995 during the Great Hanshin Earthquake serious damage occurred to port and harbour facilities at Kobe Port Island and Rokko Island. Both of these areas were reclaimed land which were filled with a crushable residual granite soil, Masado (Inagaki et al 1996; Hyodo et al 1997). In 1997 during the Kagoshima-ken Hokuseibu earthquake, the liquefaction of a crushable volcanic soil, Shirasu, was observed. Research until now has concentrated on hard grained soils tested at relatively low stresses outside the crushing region. Hyodo et al. (1998) have carried out monotonic and cyclic undrained triaxial tests to determine the liquefaction characteristics and cyclic strength of crushable soils. It was clear from the authors' previous work that not only the initial density but also the initial effective confining pressure was important in governing the cyclic behaviour. It was also evident that some particle crushing was occurring during these undrained tests. Since for weak grained soils particle crushing occurs even at low stresses, the authors decided to carry out tests on a hard grained sand over a wide range of stresses to distinguish non-crushing and crushing behaviours. Samples were therefore sieved not only before and after but also at intermediate stages of undrained monotonic and cyclic shear tests at low and high confining stresses to establish the degree of crushing that had occurred.

## 2 MATERIAL AND TESTING METHODS

Aio sand ( $G_s = 2.633$ ;  $e_{max} = 0.958$ ;  $e_{min} = 0.582$ ;  $U_c = 2.74$ ), a beach sand from Yamaguchi prefecture, was prepared with a particle size distribution of 2mm down to 74 $\mu$ m. Triaxial specimens of 50mm diameter and 100mm height were air pluviated to a relative density of 80% and an initial dry density  $\gamma_d = 1.59$  Mg/m<sup>3</sup>. The sample was saturated under a back pressure of 200kPa to a B value > 0.96. Samples were isotropically consolidated at mean normal effective stresses of 0.1MPa, 1MPa, 3MPa and 5MPa. Monotonic triaxial shear tests were carried out at confining pressures of 0.1MPa, 1MPa, 3MPa and 5MPa while cyclic triaxial tests were carried out at confining pressures of 0.1MPa, 3MPa and 5MPa with a frequency of 0.05Hz. Samples were sieved before and after testing to determine the degree of particle breakage.

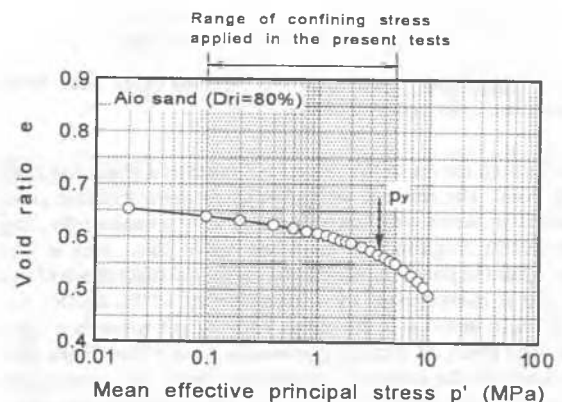


Figure 1. Isotropic compression curve for Aio sand.

The isotropic consolidation curve for these samples from 0.02MPa to 10MPa is shown in Fig.1. The yield point, given by the point of maximum curvature, is marked on this diagram at about 3MPa. It is considered that at stresses greater than 3MPa, considerable particle crushing was initiated.

## 3 UNDRAINED MONOTONIC SHEAR

Undrained compression and extension tests were carried out at each confining pressure. The stress strain plots for each test are shown in Fig. 2(a). The phase transformation points are indicated on both the compression and extension curves. The corresponding effective stress paths plotted in  $p'$ - $q$  space are shown in Fig. 2(b). At the low confining stress of 100kPa dilative behaviour was predominant and the sand behaved like a heavily overconsolidated or dense material as the stress path moved rapidly to the right from the initial stages of the test and terminated on the steady state line as shown. As the initial confining pressure was increased the stress path could be characterised by three stages. Initially relatively low positive pore pressures are produced and the stress path moves to the right indicating a dilative tendency, in the second stage the compressive behaviour predominates and

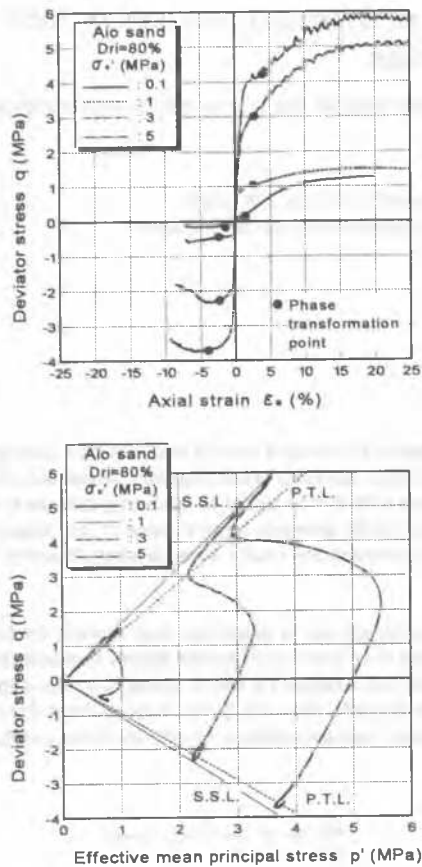


Figure 2. Stress-strain relationships and effective stress paths from monotonic tests under various confining stresses

the stress path moves to the left until it reaches a phase transformation point. The strain at which the phase transformation point is reached increases with increasing confining pressure reflecting the increasing magnitude of the compressive phase seen in this figure. After the phase transformation point the third phase of the behaviour is characterised by a strengthening of the dilative behaviour once again and the stress path moves towards a final steady state point. At confining pressures greater than 3MPa (the yield stress on the isotropic compression curve) the stress path terminates on the steady state line with large positive pore pressures and an effective  $p'$  less than the initial confining pressure indicating net compressive behaviour as would be expected of a normally consolidated material. On the other hand the stress paths on the compression side for initial confining stresses of 1MPa or greater have compressive characteristics.

#### 4 UNDRAINED CYCLIC SHEAR CHARACTERISTICS

Fig. 3 shows the relationship between cyclic deviator stress and axial strain for a confining pressure of 0.1MPa. In this case most of the axial strain occurred in extension which is characteristic of dense sands tested at low confining pressures. This type of behaviour also indicates inherent anisotropy in the sand. Fig.4 shows a similar plot for a cyclic test at 3MPa confining pressure. Here the development of cyclic strains occurs in both compression and extension. The behaviour is very reminiscent of that for clays. Examination of the cyclic stress paths for  $\sigma'_3=100\text{kPa}$  in Fig.3 shows cyclic mobility occurring as the stress paths cycle through zero effective confining pressure. In the case of  $\sigma'_3=3\text{MPa}$  the mean normal effective stress does not reach zero during each cycle. Defining cyclic failure as a strain double amplitude of 5% ( $\epsilon_{DA}=5\%$ ), cyclic strength curves have been drawn for each confining pressure and are shown in Fig.5. It can be seen that the cyclic strength decreases as the confining pressure

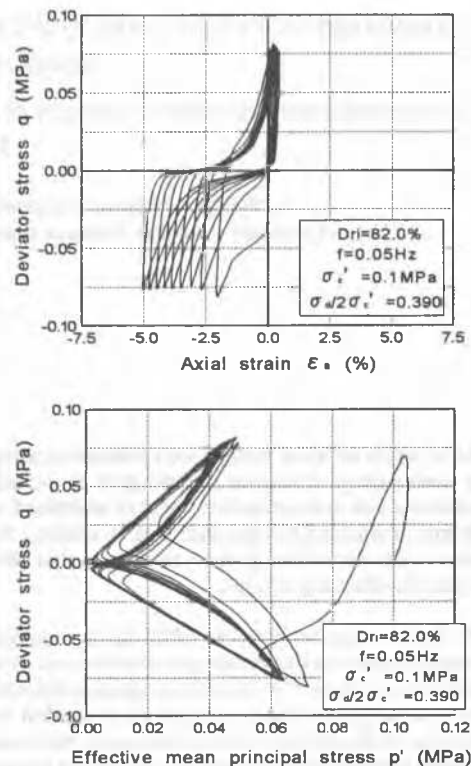


Figure 3. Typical cyclic stress and axial strain curve and effective stress path for a test at  $\sigma'_3=0.1\text{MPa}$

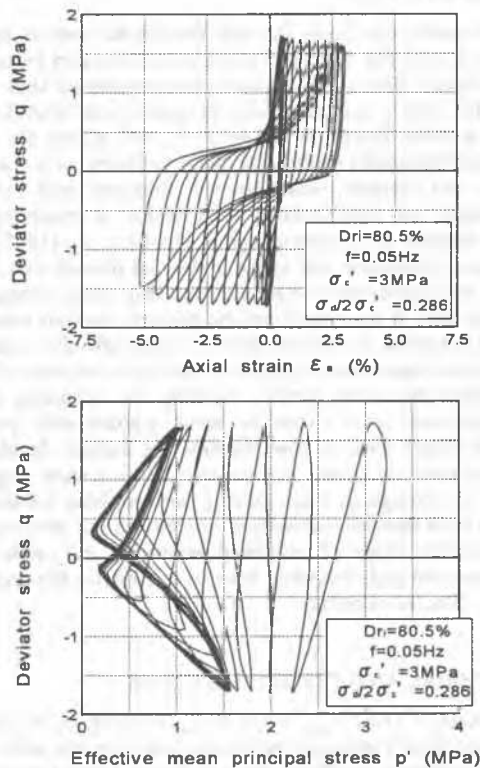


Figure 4. Typical cyclic stress and axial strain curve and effective stress path for a test at  $\sigma'_3=3\text{MPa}$

is increased from 0.1MPa to 5MPa. The cyclic strength curve is steep for a confining pressure of 100kPa, which is typical of dense sand. As the confining pressure increases to 5MPa, so the curves become flatter which is more like the behaviour of loose sand.

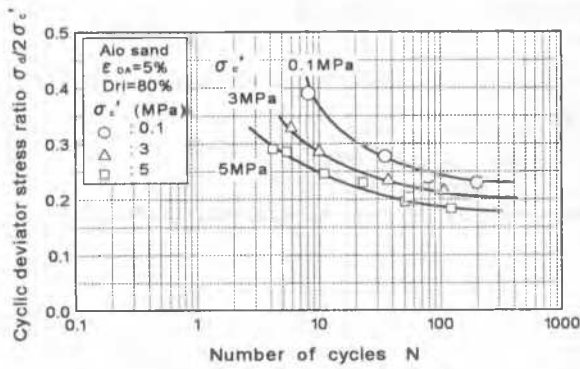


Figure 5. Cyclic strength curves for various confining stresses

### 5 PARTICLE CRUSHING UNDER MONOTONIC AND CYCLIC SHEAR STRESSES

In this study a method of evaluating particle crushing originally proposed by Miura and Yamanouchi (1971) was used. The method involves the quantification of the surface area of the particles. The specific surface of the particles was measured by first sieving the soil using 840 $\mu\text{m}$ , 420 $\mu\text{m}$ , 250 $\mu\text{m}$ , 105 $\mu\text{m}$  and 74 $\mu\text{m}$  sieve sizes. Sieving tests were carried out: 1) on the virgin samples; 2) after the end of consolidation; 3) after the phase transformation point; and 4) finally after the steady state point was reached. Additional sieving tests were also carried out at 10% and 15% axial strains. The particle surface area was then evaluated using the method described above. Thus Fig.6 which shows data for the full range of tests on the isotropically consolidated samples indicates an increase in surface area at the phase transformation state particularly at high effective confining stresses. After the phase transformation point the degree of particle crushing accelerated and continued to increase up to the steady state. In Fig.7 the contours of axial strain have been drawn for the shear tests. Up to the phase transformation line (PTL) they are initially quite curved and widely spaced but after the PTL they become straighter and as might be expected more closely spaced. Up to 0.5% strain the stress paths are dilative and only very small amounts of crushing occur in this region. Up to this point there is little breaking of asperities and the magnitude of the strain can be accounted for by particle rearrangements with movements of the same order as small asperities. It should also be noted that the degree of dilatancy increased with effective consolidation stress and hence density. From 0.5% to the PTL at 3% to 4% strain the stress paths became compressive. Over this region it is postulated that there was some breaking of small asperities. From the PTL line to the steady state the direction of the stress paths became dilative and axial strains greater than 10% were measured. It is thought that this third phase was accompanied by major particle breakage and rearrangement, particularly at higher confining stresses.

In order to observe the development of particle crushing during a cyclic loading test, a number of tests were carried out which were terminated either after a given number of cycles or when certain critical stages were reached such as the phase transformation line or a 5% double amplitude strain as shown in Fig.8 which shows the termination point for each test. This figure also includes the line showing the relationship between cyclic deviator stress ratio and the number of cycles to reach a  $\epsilon_{DA} = 5\%$ . These tests were carried out at an effective confining pressure of 5MPa which is well above the soils yield stress. Fig.9 shows the cyclic stress paths for tests terminated after 1 cycle, phase transformation and liquefaction together with

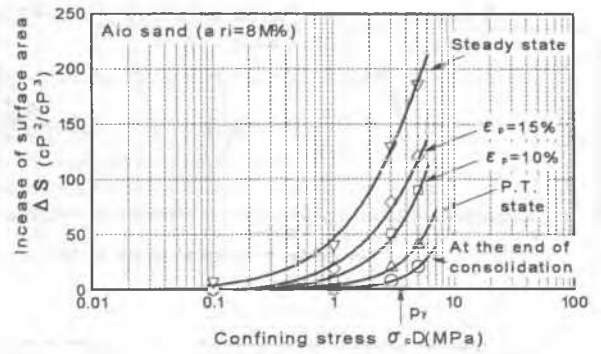


Figure 6. Increase of surface area during undrained shear with various confining stresses

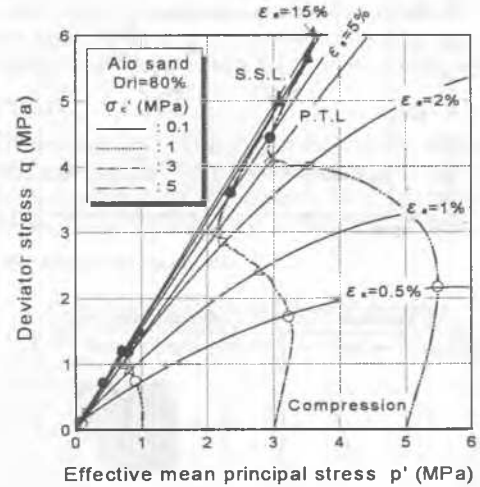


Figure 7. Contours of axial strain for undrained shear tests with various confining stresses

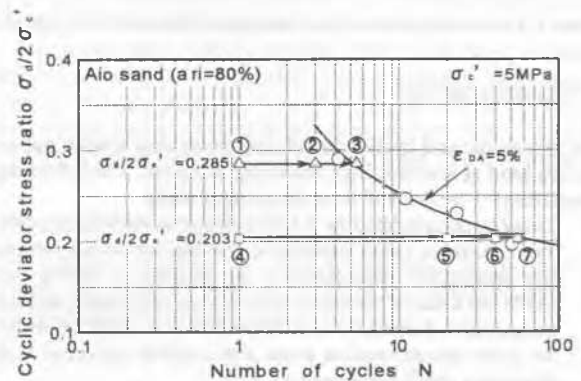


Figure 8. Relationship between cyclic deviator stress ratio and number of cycles to reach  $\epsilon_{DA} = 5\%$  and the points at which the separate tests were terminated to measure particle crushing

the development of the surface area  $S$  for all the different tests shown in Fig.8. The stress paths for tests 1,2 and 3 at a relatively high cyclic deviator stress ratio  $\sigma_d/2\sigma'_c = 0.285$  contrast with those for tests 4, 6 and 7 where  $\sigma_d/2\sigma'_c = 0.203$  and the development of the phase transformation and liquefaction was more gradual. In this figure the development of the phase transformation and  $\epsilon_{DA} = 5\%$  states are shown on the surface area plot by dotted lines. The degree of particle crushing as might be expected increased with increasing cyclic stress ratio. It can also be seen that after the phase transformation state was reached the particle surface area increased rapidly. This was because after the phase transformation point large strains occurred with associated translation and rotation of particles causing the higher degree of crushing.

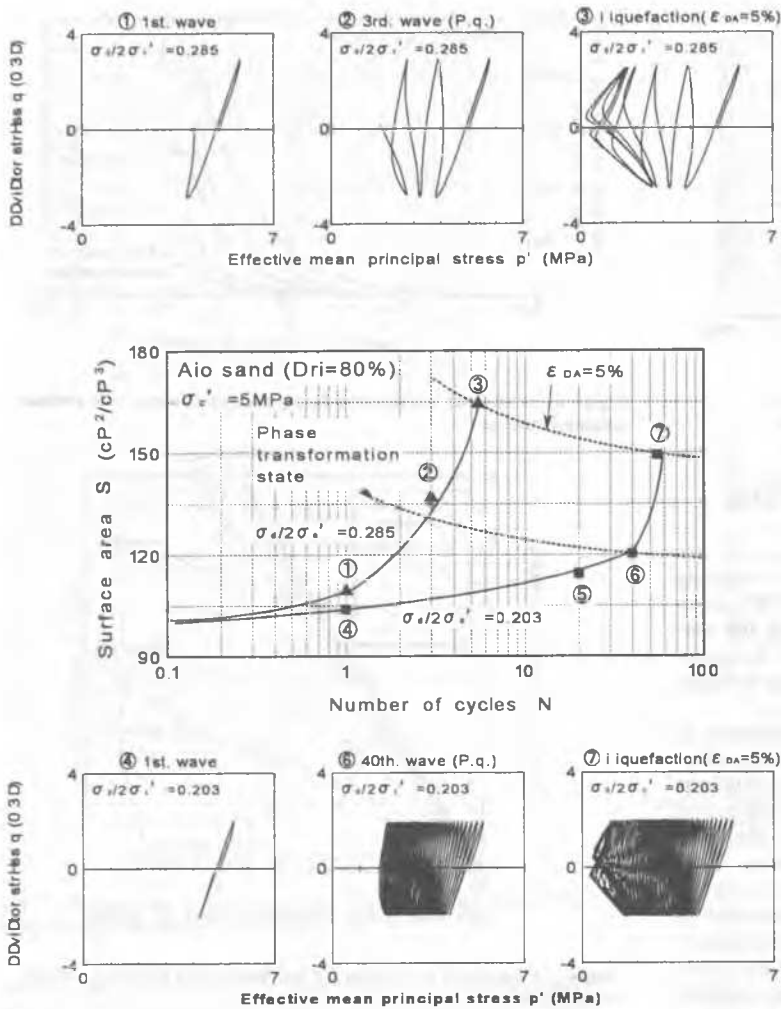


Figure 9. Relationship between grain surface area and number of cycles during undrained cyclic shear tests

## 6 CONCLUSIONS

The monotonic and cyclic triaxial tests have been carried out on a silica sand at low and high confining stresses. The following conclusions were derived from the present study.

- 1) Samples consolidated to 0.1MPa demonstrated strong dilative behaviour under monotonic loading for both isotropic and anisotropic consolidation. At stresses of 3MPa and 5MPa the dilative behaviour was largely suppressed and net compressive behaviour was observed. The strain at which the phase transformation point was reached increased with increasing confining pressure
- 2) For the high isotropic confining stresses the cyclic strength decreases with increasing confining stress as the sand behaviour becomes more like that of a loose material.
- 3) Under isotropic compression the particle surface area increased rapidly after the yield stress was exceeded. Shearing caused a marked increase in the degree of particle crushing relative to isotropic compression.
- 4) Surface area measurements were also carried out on several samples where the tests were terminated after one cycle, after the phase transformation line and when a double amplitude strain  $\epsilon_{DA} = 5\%$  was reached. The surface area and hence crushing was seen to increase rapidly for tests taken past the phase transformation state.

## REFERENCE

Hyodo, M. et al. 1997. Undrained cyclic shear characteristics of decomposed granite soil in Rokko Island, *Proc. JSCE*,

No.582/III-41, pp.87-98.

- Hyodo, M., Hyde, A.F.L. & Aramaki, N. 1998. Liquefaction of crushable soils, *Geotechnique*, Vol.48, No.4, pp.527-547.
- Inagaki, H., Iai, S., Sugano, T., Yamazaki, H. & Inatomi, T. 1996. Performance of caisson type quay walls at Kobe Port, *Soils and Foundations, Special Issue*, pp.109-118, 1996.
- Miura, N. & Yamanouchi, T. 1971. Drained shear characteristics of Toyoura sand under high confining stress, *Proc. JSCE*, No.260, pp.69-79.